CRYSTAL GROWTH & DESIGN

Article

pubs.acs.org/crystal

Spontaneous Resolution in Homochiral Helical [Ln(nic)$_2$(Hnic)(NO$_3$)] Coordination Polymers Constructed from a Rigid Non-chiral Organic Ligand

Ionut Mihalcea,[†] Nicolas Zill,[†] Valeriu Mereacre,*[,‡] Christopher E. Anson,[‡] and Annie K. Powell*[,†,‡]

[†]Institute of Nanotechnology, Karlsruhe Institute of Technology, Postfach 3640, D-76021 Karlsruhe, Germany

[‡]Institute of Inorganic Chemistry, Karlsruhe Institute of Technology, Engesserstr. 15, D-76128 Karlsruhe, Germany

Supporting Information

ABSTRACT: A series of homochiral lanthanide nicotinate helical coordination polymers [Ln^{III}(nic)$_2$(Hnic)(NO$_3$)] (Ln = Eu (**1**), Gd (**2**), Tb (**3**); Hnic = nicotinic acid) has been solvothermally synthesized using nicotinic acid. In the resulting chains, chirality is not induced by a chiral agent but appears spontaneously *via* intrachain hydrogen bondings. Compounds **2** and **3** were magnetically characterized, and luminescent properties were observed for compounds **1** and **3**.

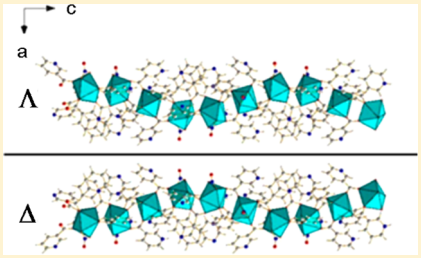

INTRODUCTION

In the past decade increasing importance has been attached to research aimed at producing chiral inorganic materials, from which the class of coordination polymers (CPs), including metal−organic frameworks (MOFs), has given the most spectacular results. The importance of this class of hybrid inorganic/organic compounds does not consist only in the endless variety of architectures and topologies but also in the photoluminescent,[1−5] magnetic,[6,7] adsorption,[8,9] and ferroelectric[10,11] properties that these materials can show and in their possible applications in nonlinear optics, asymmetric catalysis, enantioselective separation, etc.[12]

So far three general methods are known for the synthesis of homochiral CPs. The first and most popular involves using an enantiopure ligand, which by chiral conservation will give the same handedness to the final framework. However, this method has a few downsides such as the high cost of the ligands, the rather limited pool of chiral linkers, and also the possibility of in situ ligand racemization during the framework synthesis. Chiral conservation has been reviewed by Crassous in 2008,[13] and since then, the field has continued to expand.[2,14]

The second method uses non-chiral ligands, and the chirality is induced in the CP during the synthesis by a chiral agent. This agent can be an enantiopure chiral solvent, a chiral catalyst, or an enantiopure chiral auxiliary ligand that does not directly participate in the formation of the framework but forces the structure to adopt a chiral topology. This method can have the same drawbacks as the first. Large contributions to this field have been made by Morris and Bu[9,15] as well as other research groups.[7,16]

The third method uses only non-chiral starting materials, and the chirality appears by spontaneous resolution during the crystallization of the complex. This can be generated and supported by different factors such as ligand conformation and flexibility, metal coordination number, coordination sphere geometry, and supramolecular interactions such as hydrogen bond and $\pi-\pi$ stacking interactions. The spontaneous resolution is unpredictable, and generally the products are conglomerates, racemic mixtures of enantiopure crystals. The so-called helicates, a specific class of coordination polymers containing large, highly flexible, organic ligands that are capable of wrapping around the axially disposed metal centers in order to generate helical chirality, have largely been synthesized using this method. Important contributions in this field have been made by the groups of Piguet and Williams,[3,17] although helicates have been reported by other research groups[4,18] and been the subject of several review articles.[19]

Another class of chiral complexes obtained through spontaneous resolution is represented by compounds containing small rigid organic molecules as ligands. These ligands cannot themselves adopt a helical conformation, so that the predictability of obtaining such structures is low. Although many such compounds have been reported,[5,11,20] the mechanism behind the noncentrosymmetric self-assembly into chiral complexes remains elusive.

The series of new lanthanide nicotinates [Ln(nic)$_2$(Hnic)(NO$_3$)] (Ln = Eu (**1**), Gd (**2**), Tb (**3**); Hnic = nicotinic acid) described in this work belongs to this latter class. All three CPs are isostructural, crystallizing in the enantiomeric pair of hexagonal chiral space groups P6$_1$/P6$_5$ with $Z = 6$ and were solvothermally synthesized from the corresponding nitrate metal salt and the nonchiral ligand nicotinic acid in acetonitrile. In what follows we discuss the factors inducing the spontaneous resolution. Furthermore, the thermal stability of the com-

Received: June 6, 2014
Revised: August 6, 2014
Published: August 8, 2014

   dx.doi.org/10.1021/cg500827u | *Cryst. Growth Des.* 2014, 14, 4729−4734

pounds was investigated, and for compounds **2** and **3**, the magnetic properties were also investigated. For compounds **1** and **3**, the fluorescent properties were also investigated.

EXPERIMENTAL SECTION

All materials and reagents are commercially available and have been used without further purification. Elemental (C, H, N) analyses were performed on an Elementar Vario EL analyzer. Infrared (IR) samples were prepared as KBr pellets, and spectra were obtained in 4000−400 cm^{-1} range using a PerkinElmer Spectrum One spectrometer. Thermogravimetric analysis (TGA) experiments were conducted on a Netzsch STA 409c thermogravimetric analyzer with the heating rate of 5 °C/min from 20 to 800 °C under dry air atmosphere. Powder X-ray diffraction (PXRD) investigations were conducted on a STOE Stadi P X-ray diffractometer with Cu Kα1 radiation. Photoluminescent spectra were recorded on a spectrofluorometer Fluorolog FL3-22 (HORIBA JobinYvon) equipped with a 450 W xenon lamp for the excitation source, excitation and emission double-grating monochromators, a TBX-04 detector, and a KV 370 (Schott AG) long-pass filter.

Synthesis of [Eu(nic)$_2$(Hnic)(NO$_3$)] (1). A mixture of $Eu(NO_3)_3 \cdot 6H_2O$ (0.447 g, 1 mmol), Hnic (0.246 g, 2 mmol), and CH_3CN (10 mL) was sealed in a 23 mL Teflon-lined stainless-steel autoclave and heated to 120 °C during 72 h and then cooled to room temperature at 10 °C/h. Yellow needle-shaped crystals were isolated by filtration and washed with dry acetonitrile, in a yield of 49% (based on Eu).

Calcd for $C_{18}H_{13}EuN_4O_9$: C, 37.19; H, 2.25; N, 9.64. Found: C, 36.68; H, 2.21; N, 9.85. IR (KBr cm^{-1}): 3083(w), 3057(w), 1646(m), 1609(s), 1592(s), 1573(m), 1550(m), 1470(s), 1422(s), 1408(s), 1304(s), 1033(w), 850(w), 760(m), 696(w), 540(w), 416(w).

Synthesis of [Gd(nic)$_2$(Hnic)(NO$_3$)] (2). Compound **2** was synthesized from $Gd(NO_3)_3 \cdot 6H_2O$ (0.452 g, 1 mmol) in a yield of 62% (based on Gd).

Calcd for $C_{18}H_{13}GdN_4O_9$: C, 36.86; H, 2.23; N, 9.55. Found: C, 35.79; H, 2.24; N, 9.94. IR (KBr cm^{-1}): 3083(w), 3058(w), 1648(m), 1610(s), 1593(s), 1573(m), 1550(m), 1472(s), 1423(s), 1409(s), 1305(s), 1034(w), 851(w), 760(m), 696(w), 542(w), 416(w).

Synthesis of [Tb(nic)$_2$(Hnic)(NO$_3$)] (3). Compound **3** was synthesized from $Tb(NO_3)_3 \cdot 6H_2O$ (0.453 g, 1 mmol) in a yield of 41% (based on Tb).

Calcd for $C_{18}H_{13}TbN_4O_9$: C, 36.75; H, 2.23; N, 9.52. Found: C, 36.06; H, 2.17; N, 9.70. IR (KBr cm^{-1}): 3082(w), 3057(w), 1648(m), 1610(s), 1593(s), 1574(m), 1550(m), 1471(s), 1423(s), 1409(s), 1305(s), 1034(w), 850(w), 760(m), 696(w), 543(w), 417(w).

Fully recorded IR spectra of the compounds can be found in Figure S1, Supporting Information.

Magnetic Measurements. Magnetic susceptibility measurements were obtained with a Quantum Design SQUID magnetometer MPMS-XL. dc susceptibility measurements were made over the temperature range 1.8−300 K under applied fields of 0.1 T. Magnetization was measured with fields 0−7 T. Measurements were performed on polycrystalline samples restrained in Apiezon grease. The magnetic data were corrected for the sample holder and the diamagnetic contribution.

X-ray Data Collection and Structure Refinement. Data for **1**−**3** were collected at 100(2) K on a Bruker SMART Apex CCD diffractometer using graphite-monochromated Mo-K_α radiation. Data were corrected for absorption using SADABS.[21] Structures were solved by dual-space direct methods (SHELXT) and full-matrix least-squares refinement against F^2 using all data (SHELX-2013).[22] All non-H atoms were refined anisotropically. H atoms bonded to C were placed in calculated positions using a riding model; the coordinates of H(2), forming the hydrogen bond between N(2) and N(1′), were refined, while its isotropic temperature factor was either refined (**1** and **3**) or set at 1.2(U_{eq}) for N(2) (**2**). The refinements for **2** and **3** indicated a small degree (13% and 16%, respectively) of merohedral twinning (by 180° rotation about (**a** + **b**), which was modeled with a "TWIN 0 1 0 1 0 0 0 −1 2" instruction). In both cases, this merohedral twinning was first tested by refining with a "TWIN 0 1 0 1 0 0 0 0 −1 −4" instruction, which confirmed that in each case the minor merohedrally twinned domain was of the same enantiomer as the major domain.

Crystallographic data and structure refinement parameters for **1**−**3** are summarized in Table 1.

Table 1. Crystallographic Data for Compounds 1−3

	1	2	3
	$C_{18}EuH_{13}N_4O_9$	$C_{18}GdH_{13}N_4O_9$	$C_{18}H_{13}N_4O_9Tb$
FW (g mol^{-1})	581.28	586.57	588.24
T (K)	100(2)	100(2)	100(2)
crystal system	hexagonal	hexagonal	hexagonal
space group	$P6_5$	$P6_1$	$P6_1$
a (Å)	11.1955(3)	11.1905(3)	11.1793(3)
c (Å)	26.7384(14)	26.6938(15)	26.6236(15)
V (Å^3)	2902.4(2)	2894.9(3)	2881.6(2)
Z	6	6	6
D_{calc} (g cm^{-3})	1.995	2.019	2.034
μ [Mo-K_α] (mm^{-1})	3.305	3.500	3.745
F(000)	1704	1710	1716
data collected	38104	31992	21431
R_{int}	0.0276	0.0318	0.0293
unique data	4568	4368	4353
data with $I > 2\sigma(I)$	4504	4358	4336
parameters	294	293	294
wR_2 (all data)	0.0387	0.0393	0.0449
S (all data)	1.051	1.042	1.018
R_1 [$I > 2\sigma(I)$]	0.0159	0.0166	0.0186
extent merohedral twinning (see text)	0.0004(1)	0.1289(5)	0.1595(6)
flack χ parameter	−0.025(5)	−0.023(5)	−0.012(9)
largest diff. peak/hole (e A^{-3})	+0.87/−0.38	+0.58/−0.32	+0.63/−0.45

Crystallographic data (excluding structure factors) for the structures in this article have been deposited with the Cambridge Crystallographic Data Centre as supplementary publication nos. CCDC 997749−997751. Copies of the data can be obtained, free of charge, on application to CCDC, 12 Union Road, Cambridge CB2 1EZ, U.K.; http://www.ccdc.cam.ac.uk/cgi-bin/catreq.cgi; e-mail data_request@ccdc.cam.ac.uk; or fax +44 1223 336033.

RESULTS AND DISCUSSION

Synthesis. Formation of the 1D Chiral Chains. The employed synthetic route was solvothermal using CH_3CN as solvent, corresponding nitrate lanthanide salts as metal source, and nicotinic acid as ligand.

After a quick look in the literature over the chiral CPs obtained by spontaneous resolution from rigid ligands, one can assemble a list of guidelines for ligand selection to improve the predictability of chiral architecture formation: the organic molecule should be asymmetric (lack of any molecular symmetry elements except E), should possess a rather small number of coordination groups disposed unilateral on the molecule, and also should possess functional groups capable of generating weak forces such as hydrogen bonds and/or $\pi-\pi$ stacking interactions that will stabilize the chiral motif.

In our work the nicotinic acid was selected as ligand of choice for several reasons: it is commercially available and corresponds to the above-mentioned ligand selection rules, and although there are around 90 hits in CCDC of lanthanide nicotinates, none of the compounds is chiral. Also it has been observed that

dx.doi.org/10.1021/cg500827u | Cryst. Growth Des. 2014, 14, 4729−4734

the metal source plays an important role in synthesis; essays of employing various lanthanide salts different from nitrate generated $[Ln(nic)_3H_2O]$ dinuclear molecular complex, already mentioned in literature.[23] Even attempts of replacing the chelating nitrate group with another ligand molecule or with the molecule of a monocarboxylic coligand (formic, acetic, and benzoic acids) have failed giving the chiral phase reported in this article impurified either by the hydrated molecular complex or by unidentified powder products.

Crystal Structure. All three compounds **1** to **3** crystallize isotypically in one or other of the hexagonal $P6_1/P6_5$ enantiomeric pairs of chiral space groups, with $Z = 6$. The two space groups correspond to the $P(\Delta)$ and the $M(\Lambda)$ enantiomers, respectively. The structure of the europium analogue **1** will be described here; the other two compounds are closely isostructural.

As shown in Figure 1, adjacent Eu centers within the polymeric chain are linked by three nicotinate carboxylate groups, all bridging in the *syn*–*syn* coordination mode. The crystallographically independent Eu(1) is thus ligated by six carboxylate oxygen atoms, each from a different organic ligand. The O_8 coordination environment of Eu(1) is completed by a chelating nitrate ligand, with the eight oxygen atoms describing a rather regular dodecahedral geometry (Figure 2). The dodecahedron is slightly elongated along a 2-fold axis passing through Eu(1) and the nitrate nitrogen and approximates to C_{2v} local symmetry, if only the carboxylate oxygen atoms and nitrate ligand are taken into account. The Eu(1)–O bond lengths range from 2.308(2) to 2.439(2) Å for the carboxylate oxygen atoms, with the distances to the two nitrate oxygen atoms rather longer at 2.497(2) and 2.525(2) Å.

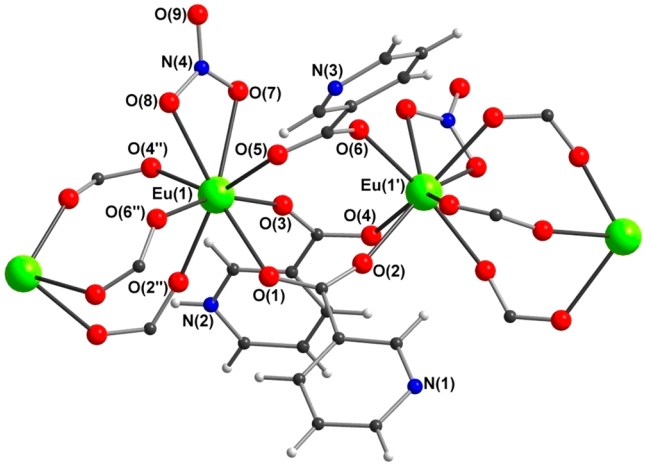

Figure 1. Coordination environment of Eu(1) in **1** and the linkages between adjacent Eu centers (symmetry codes: $'x - y, x, z - 1/6$; $''y, x + y, z + 1/6$).

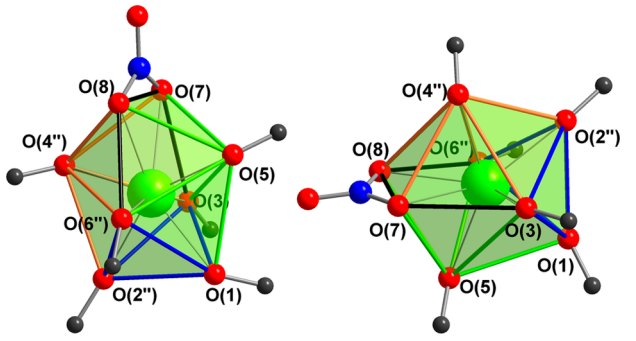

Figure 2. Dodecahedral coordination polyhedron for Eu(1) in **1**: side view (left) and viewed down the local 2-fold axis (right).

In order to maintain charge neutrality, one of the nicotinate nitrogen atoms, N(2), is protonated. This hydrogen atom, H(2), which could be located and fully refined, then forms a hydrogen bond to N(1) from the ligand in the next-but-one link in the chain, with N(2)···N(1′) 2.706(5) Å and N(2)–H(2)···N(1′) 171(5)°. The presence of the chelating nitrate in the coordination shell of Eu(1) results in a nonlinear Eu(1′)···Eu(1)···Eu(1″) angle of 158.7° (Figure 1). Given that the effect of the intrachain hydrogen bonding is to pull two organic ligands from next-nearest links in the polymeric chain closer together and that these hydrogen bonds are also displaced to either side of the local plane defined by these three metal atoms, their effect is to pull the coordination polymer into a helical configuration (Figure 3).

The result is a 6-fold helix, in which the Eu···Eu distance between adjacent metal centers in the chain is 4.7797(2) Å, while the pitch of the helix is given by the unit cell *c* parameter, 26.7384(14) Å. If one considers the coordination polyhedron in Figure 2, the three carboxylate oxygen atoms O(1), O(3), and O(5), from the carboxylates of one link in the chain, form a nearly equilateral triangle. The oxygen atoms O(2″), O(4″), and O(6″), from the corresponding respective carboxylates forming the linkage on the other side of Eu(1), form a similar equilateral triangle in the coordination polyhedron. The planes of these two triangles are close to parallel, but the triangles are mutually rotated to give a "star-of-David" motif when viewed along the chain. This rotation of one linkage relative to the next of ca. 60°, which thus appears to be a consequence of the dodecahedral coordination of Eu(1), immediately leads to the 6-fold nature of the helix.

For each of the crystal structures reported here, the measured crystal was found to be enantiomerically pure, with the final value of the Flack χ parameter having a magnitude of no more than 0.032 (see Table 1). All the helices in a given crystal thus have the same handedness, either all having a right-handed thread or all being left-handed. The space groups $P6_5$ and $P6_1$ form an enantiomeric pair, and within a given batch of crystals, there will be a statistical 1:1 mixture of crystals corresponding to each of the two space groups. Among the three crystal structures reported here, one involves crystallization in $P6_5$ and two in $P6_1$. Two of the structures reported here showed a small degree of merohedral twinning; in each case this was shown to involve a 180° rotation about the (**a** + **b**) vector, rather than a reflection (see experimental section), and therefore does not affect the enantiomeric purity of the crystals concerned.

In addition to the intrachain N–H···N hydrogen bonding, the crystal packing is stabilized by a number of C–H···O interchain interactions. These, involving nicotinate and nitrate ligands from adjacent chains, have C···O distances in the range 3.111–3.505 Å. This results in a rather dense packing of the chains (Figure 4), in which there is no space between the chains for any lattice solvent molecules.

By analyzing the large number of reported chiral CPs that exhibit helix architecture, it can be observed that the structure of most of them (around 64%) are exhibiting only 2- and 3-fold screw axes; the CPs exhibiting high symmetry 4-fold screw axes are rather few (about 22%), and even scarcer (only 14%) are the number of compounds containing in their structure 6-fold

dx.doi.org/10.1021/cg500827u | *Cryst. Growth Des.* 2014, 14, 4729–4734

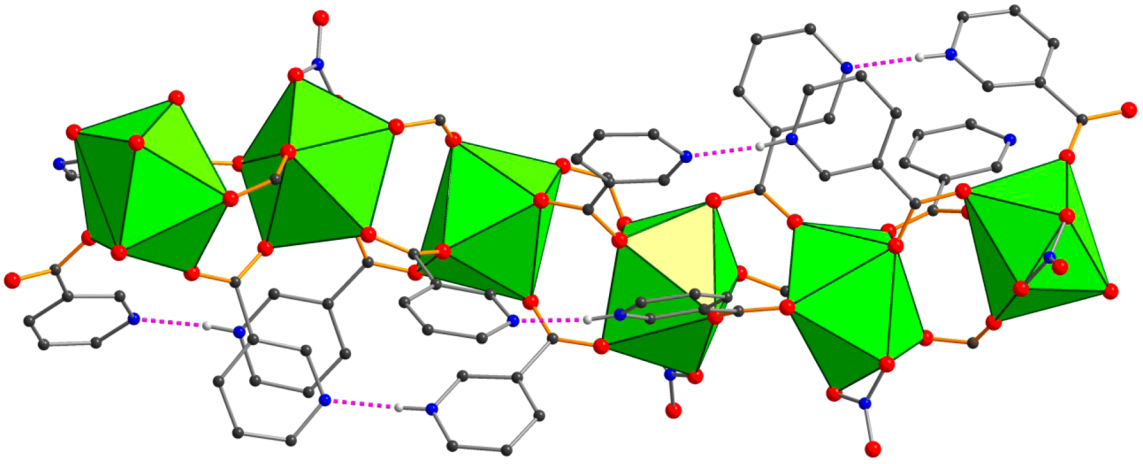

Figure 3. Relationship between the N−H···N hydrogen bonding (shown as purple dashed lines) and the helical structure of the polymer. The pyridyl ring of the ligand containing N(3) (not involved in hydrogen bonding) is omitted for clarity.

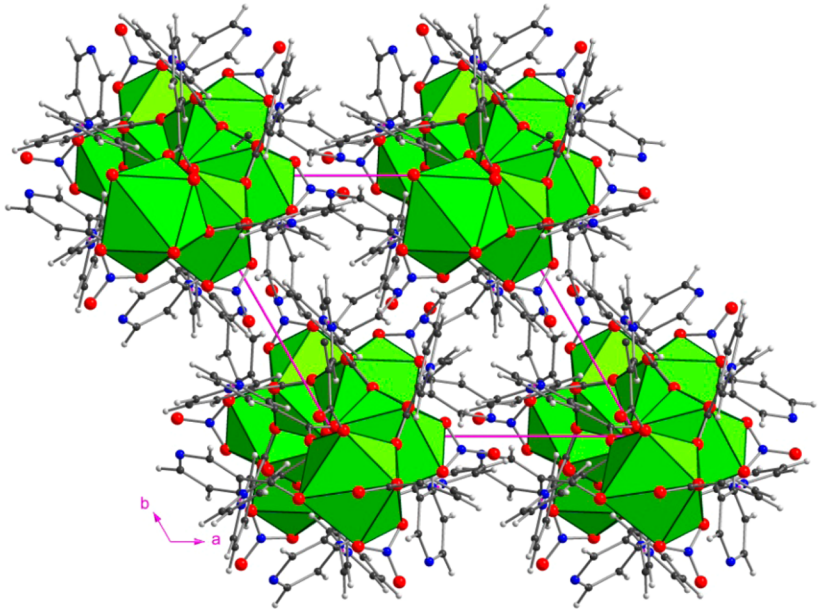

Figure 4. Packing of the $[Eu(nic)_2(Hnic)(NO_3)]$ chains in the crystal of **1**, viewed along the *c* axis.

screw axes. In this work, we report a series of rare CPs exhibiting $6_1/6_5$ screw axes.

Thermal Properties. All three compounds present similar thermal degradation patterns. The TG curves of **1**−**3** show two main decomposition steps. The first one occurring at 290 °C is steep, while the second one occurring around 500 °C is smoother suggesting a longer process. At 800 °C, all four compounds are decomposed into the corresponding lanthanide oxide form giving total weight losses of 69.5%, 68.6%, and 68.2% for **1**, **2**, and **3**, respectively (expected values of 69.7%, 69.1%, and 68.9%). The existence of the two degradation steps can be attributed to the oxidizing properties of the nitro group playing the role of comburant and accelerator for the partial degradation of the ligand molecules. This accelerated oxidation is responsible for the first weight loss. The second one, a process with a slower kinetic, has been attributed to the normal oxidation in air of the organic ligand giving the final oxide form.

Magnetic Properties. The dc magnetic susceptibility properties of compounds **2** and **3** were investigated in the temperature range 1.8−300 K (Figure 5); compound **1** was not

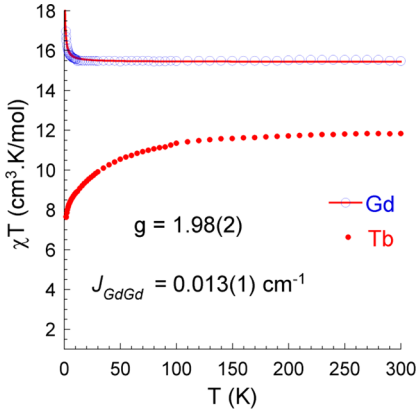

Figure 5. Temperature dependence of the χT product at 1000 Oe for **2** and **3**. Inset: the best fit parameters for the Gd compound.

investigated due to the diamagnetic low-spin $^7F_0$ ground state of the Eu^{III} ion. The field dependence of the magnetization for the complexes between 2 and 5 K are shown in Figure S4,

dx.doi.org/10.1021/cg500827u | *Cryst. Growth Des.* 2014, 14, 4729−4734

Supporting Information. At 300 K, the χT values of complexes **2** and **3** are 7.7 and 11.8 cm^3 K mol^{-1}, respectively, in good agreement with the theoretical values (**2**, 7.88 for $^8S_{7/2}$, $g = 2$; **3**, 11.82 for $^7F_6$, $g = 3/2$) for noninteracting lanthanide ions.[24]

The χT values for compound **2** stay almost constant with decreasing temperature from 300 K down to approximately 10 K, below which χT increases considerably, reaching a value of 17.0 cm^3 K mol^{-1} at 1.8 K, indicating ferromagnetic coupling between the Gd^{III} ions within the polymeric chains. The experimental data for the compound **2** were fitted to a model based on the isotropic spin Hamiltonian $H = -J(2S_{Gd})$, obtaining $J/k_B = 0.013(1)$ cm^{-1} and $g = 1.98(2)$, in good agreement with previous studies.[25] Magnetization measurements performed at low temperatures reveal a saturation of 6.8 μ_B at 7 T, in good agreement with the expected value of 7.0 μ_B (for $g = 2.00$).

For compound **3**, the thermal variation of χT shows a decrease at lower temperatures, reaching a value of 7.6 cm^3 K mol^{-1} at 1.8 K. For such a lanthanide ion with an unquenched orbital moment, the decrease of the χT can originate from several contributions, like antiferromagnetic interactions, magnetic anisotropy, and/or thermal depopulation of the Stark sublevels. The linear variation and nonsaturation of the magnetization (Figure S4, Supporting Information) indicate the presence of large magnetic anisotropy and/or low-lying excited states. The value of the magnetization at 7 T is ~4.8 μ_B. The considerable variation from the expected magnetization saturation values points to strong contribution from the ligand field.

Photoluminescent Properties. Considering excellent luminescent properties of Eu^{3+} (bright red) and Tb^{3+} (green), solid-state emission spectra of Eu^{3+} (**1**) and Tb^{3+} (**3**) at room temperature are shown in Figures 6 and S5, Supporting Information. Excitation was performed in both cases at 350 nm in order to see the fluorescence emission of the nicotinic acid ligand (370−520 nm).

The characteristic five luminescent peaks of Eu^{3+} (**1**) are observed at 578 nm ($^5D_0 \rightarrow {}^7F_0$), 590 nm ($^5D_0 \rightarrow {}^7F_1$), 615 nm ($^5D_0 \rightarrow {}^7F_2$), 651 nm ($^5D_0 \rightarrow {}^7F_3$), and 696−719 nm ($^5D_0 \rightarrow {}^7F_4$). The presence of the symmetric forbidden emission $^5D_0 \rightarrow {}^7F_0$ (electric-dipole transition) indicates that Eu^{3+} ions occupy sites without inversion symmetry. The hypersensitive $^5D_0 \rightarrow {}^7F_2$ transition (electric dipole) is stronger than the $^5D_0 \rightarrow {}^7F_1$ transition (magnetic dipole), which suggests that Eu^{3+} ions have a low symmetry coordination environment. These results are in agreement with the X-ray analysis.

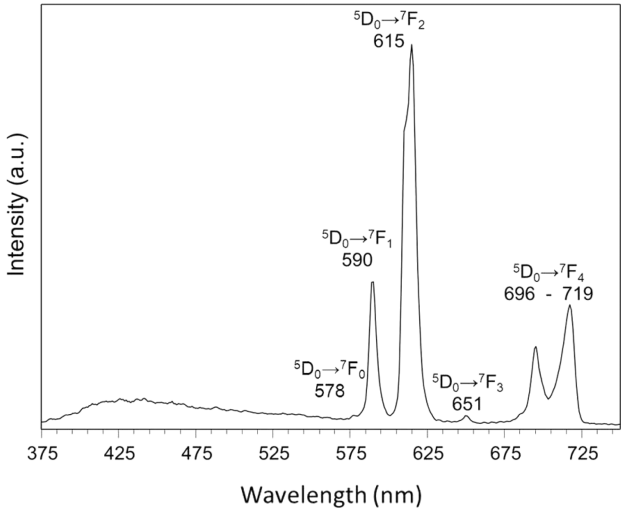

Figure 6. Room temperature, solid state emission spectrum of compound **1** excited at 350 nm.

Though less sensitive than Eu^{3+} to the chemical environment, four distinctive bands can be seen on the emission spectrum of Tb^{3+} (ii): at 487 nm ($^5D_4 \rightarrow {}^7F_6$), the hypersensitive transition $^5D_4 \rightarrow {}^7F_5$ responsible of the green luminescence at 543 nm, at 581−587 nm ($^5D_4 \rightarrow {}^7F_4$), and at 618 nm ($^5D_4 \rightarrow {}^7F_3$).

CONCLUSIONS

In this work, a series of three new isostructural lanthanide nicotinate complexes has been reported using solvothermal conditions and the commercially available nonchiral nicotinic acid as a ligand. The resulting structures appear as chiral helices induced by intrachain hydrogen bondings. Complexes with Gd^{III} (**2**) and Tb^{III} (**3**) ions show ferromagnetic and antiferromagnetic properties, respectively, whereas complex with Eu^{III} (**1**) ion could not be investigated due to the diamagnetic low-spin $^7F_0$ ground state of the europium ion. However, in comparison with compounds **2** and **3**, the europium derivative has shown characteristic photoluminescent properties suggesting that Eu^{III} ions have a low symmetry coordination environment, which is in agreement with the crystallographic analysis.

ASSOCIATED CONTENT

Supporting Information

IR, PXRD, and solid state emission spectra; TGA and magnetization curves. This material is available free of charge via the Internet at http://pubs.acs.org.

AUTHOR INFORMATION

Corresponding Authors

*(V.M.) E-mail: valeriu.mereacre@kit.edu.

*(A.K.P.) E-mail: annie.powell@kit.edu.

Notes

The authors declare no competing financial interest.

ACKNOWLEDGMENTS

This work was supported by the DFG-funded transregional collaborative research center SFB/TRR 88 "3MET".

REFERENCES

(1) Chen, Z.; Qin, S.; Liu, D.; Shen, Y.; Liang, F. *Cryst. Growth Des.* **2013**, *13*, 3389.

(2) (a) Wang, S. H.; Zheng, F. K.; Zhang, M. J.; Liu, Z. F.; Chen, J.; Xiao, Y.; Wu, A. Q.; Guo, G. C.; Huang, J. S. *Inorg. Chem.* **2013**, *52*, 10096. (b) Dong, L. J.; Chu, W.; Zhu, Q. L.; Huang, R. D. *Cryst. Growth Des.* **2011**, *11*, 93. (c) Zheng, X. D.; Zhang, M.; Jiang, L.; Lu, T. B. *Dalton Trans.* **2012**, *41*, 1786. (d) Chen, Z. L.; Qin, S. N.; Liu, D. C.; Shen, Y. L.; Liang, F. P. *Cryst. Growth Des.* **2013**, *13*, 3389. (e) Li, X. L.; Chen, C. L.; Kang, J. L.; Wang, A. L.; Wang, P. Y.; Xiao, H. P. *Inorg. Chim. Acta* **2013**, *408*, 78. (f) He, J. H.; Zhang, G. J.; Xiao, D. R.; Chen, H. Y.; Yan, S. W.; Wang, X.; Yang, J.; Yuan, R.; Wang, E. B. *J. Mol. Struct.* **2012**, *1018*, 131.

(3) (a) Piguet, C.; Bunzli, J.-C. G.; Bernardinelli, G.; Hopfgartner, G.; Williams, A. F. *J. Am. Chem. Soc.* **1993**, *115*, 8197. (b) Piguet, C.; Williams, A. F.; Bernardinelli, G.; Bunzli, J.-C. G. *Inorg. Chem.* **1993**, *32*, 4139.

(4) (a) Deiters, E.; Eliseeva, S. V.; Bünzli, J.-C. G. *Front. Chem.* **2013**, *1*, 1. (b) Wang, X. J.; Huang, T. H.; Tang, L. H.; Cen, Z. M.; Ni, Q. L.;

Gui, L. C.; Jiang, X. F.; Liu, H. K. *CrystEngComm* **2010**, *12*, 4356. (c) Feng, R.; Jiang, F. L.; Chen, L.; Yan, C. F.; Wu, M. Y.; Hong, M. C. *Chem. Commun.* **2009**, 5296. (d) Zhang, L.; Zhang, P.; Zhao, L.; Lin, S.-Y.; Xue, S.; Tang, J.; Liu, Z. *Eur. J. Inorg. Chem.* **2013**, 1351. (e) Lin, S.-Y.; Xu, G.-F.; Zhao, L.; Guo, Y.-N.; Guo, Y.; Tang, J. *Dalton Trans.* **2011**, *40*, 8213.

(5) (a) Gu, X. J.; Xue, D. F. *Inorg. Chem.* **2006**, *45*, 9257. (b) Zhou, T. H.; Zhang, J.; Zhang, H. X.; Feng, R.; Mao, J. G. *Chem. Commun.* **2011**, *47*, 8862. (c) Zhang, Q. F.; Hao, H. G.; Zhang, H. N.; Wang, S. N.; Jin, J.; Sun, D. Z. *Eur. J. Inorg. Chem.* **2013**, 1123. (d) Wang, P. Y.; Dai, S. C.; Lin, W. F.; Wu, M. F.; Yang, H. B.; Zhou, P.; Zou, J. P.; Guang, W. T.; Luo, X. B. *Inorg. Chim. Acta* **2013**, *404*, 155. (e) Chen, N.; Li, M. X.; Yang, P.; He, X.; Shao, M.; Zhu, S. R. *Cryst. Growth Des.* **2013**, *13*, 2650.

(6) (a) Lisnard, L.; Charnoreau, L. M.; Li, Y. L.; Journaux, Y. *Cryst. Growth Des.* **2012**, *12*, 4955. (b) Gil-Hernandez, B.; Hoppe, H. A.; Vieth, J. K.; Sanchiz, J.; Janiak, C. *Chem. Commun.* **2010**, *46*, 8270. (c) Gil-Hernandez, B.; Maclaren, J. K.; Hoppe, H. A.; Pasan, J.; Sanchiz, J.; Janiak, C. *CrystEngComm* **2012**, *14*, 2635. (d) Tong, X. L.; Hu, T. L.; Zhao, J. P.; Wang, Y. K.; Zhang, H.; Bu, X. H. *Chem. Commun.* **2010**, *46*, 8543. (e) Majeed, Z.; Mondal, K. C.; Kostakis, G. E.; Lan, Y. H.; Anson, C. E.; Powell, A. K. *Chem. Commun.* **2010**, *46*, 2551.

(7) Liu, Q. Y.; Xiong, W. L.; Liu, C. M.; Wang, Y. L.; Wei, J. J.; Xiahou, Z. J.; Xiong, L. H. *Inorg. Chem.* **2013**, *52*, 6773.

(8) (a) Kepert, C. J.; Prior, T. J.; Rosseinsky, M. J. *J. Am. Chem. Soc.* **2000**, *122*, 5158. (b) Chen, Z. L.; Liu, X. L.; Zhang, C. B.; Zhang, Z.; Liang, F. P. *Dalton Trans.* **2011**, *40*, 1911. (c) Anokhina, E. V.; Go, Y. B.; Lee, Y.; Vogt, T.; Jacobson, A. J. *J. Am. Chem. Soc.* **2006**, *128*, 9957. (d) Bradshaw, D.; Prior, T. J.; Cussen, E. J.; Claridge, J. B.; Rosseinsky, M. J. *J. Am. Chem. Soc.* **2004**, *126*, 6106.

(9) Zhang, J.; Chen, S. M.; Wu, T.; Feng, P. Y.; Bu, X. H. *J. Am. Chem. Soc.* **2008**, *130*, 12882.

(10) (a) Ye, Q.; Fu, D. W.; Tian, H.; Xiong, R. G.; Chan, P. W. H.; Huang, S. P. D. *Inorg. Chem.* **2008**, *47*, 772. (b) Huang, Q. A.; Yu, J. C.; Gao, J. K.; Rao, X. T.; Yang, X. L.; Cui, Y. J.; Wu, C. D.; Zhang, Z. J.; Xiang, S. C.; Chen, B. L.; Qian, G. D. *Cryst. Growth Des.* **2010**, *10*, 5291.

(11) (a) Du, F. L.; Zhang, H. B.; Tian, C. B.; Du, S. W. *Cryst. Growth Des.* **2013**, *13*, 1736. (b) Su, Z.; Chen, M. S.; Fan, J. A.; Chen, M.; Chen, S. S.; Luo, L.; Sun, W. Y. *CrystEngComm* **2010**, *12*, 2040.

(12) (a) Dybtsev, D. N.; Nuzhdin, A. L.; Chun, H.; Bryliakov, K. P.; Talsi, E. P.; Fedin, V. P.; Kim, K. *Angew. Chem., Int. Ed.* **2006**, *45*, 916. (b) Yue, Q.; Yang, J.; Li, G. H.; Li, G. D.; Chen, J. S. *Inorg. Chem.* **2006**, *45*, 4431. (c) Wu, C. D.; Hu, A.; Zhang, L.; Lin, W. B. *J. Am. Chem. Soc.* **2005**, *127*, 8940.

(13) Crassous, J. *Chem. Soc. Rev.* **2009**, *38*, 830.

(14) (a) Zhu, Q. L.; Sheng, T. L.; Fu, R. B.; Tan, C. H.; Hu, S. M.; Wu, X. T. *Chem. Commun.* **2010**, *46*, 9001. (b) Li, X. F.; Zhao, H. J.; Zeng, Q. H. *CrystEngComm* **2013**, *15*, 3593.

(15) (a) Lin, Z. J.; Slawin, A. M. Z.; Morris, R. E. *J. Am. Chem. Soc.* **2007**, *129*, 4880. (b) Zhang, J.; Chen, S. M.; Nieto, R. A.; Wu, T.; Feng, P. Y.; Bu, X. H. *Angew. Chem., Int. Ed.* **2010**, *49*, 1267. (c) Morris, R. E.; Bu, X. H. *Nat. Chem.* **2010**, *2*, 353. (d) Kang, Y.; Chen, S. M.; Wang, F.; Zhang, J. A.; Bu, X. H. *Chem. Commun.* **2011**, *47*, 4950.

(16) (a) Bisht, K. K.; Suresh, E. *J. Am. Chem. Soc.* **2013**, *135*, 15690. (b) Liu, Y. C.; Zhang, H. B.; Tian, C. B.; Lin, P.; Du, S. W. *CrystEngComm* **2013**, *15*, 5201. (c) Dai, F. N.; He, H. Y.; Zhao, X. L.; Ke, Y. X.; Zhang, G. Q.; Sun, D. F. *CrystEngComm* **2010**, *12*, 337.

(17) (a) Cantuel, M.; Bernardinelli, G.; Muller, G.; Riehl, J. P.; Piguet, C. *Inorg. Chem.* **2004**, *43*, 1840. (b) Piguet, C.; Bernardinelli, G.; Bocquet, B.; Quattropani, A.; Williams, A. F. *J. Am. Chem. Soc.* **1992**, *114*, 7440. (c) Bernardinelli, G.; Piguet, C.; Williams, A. F. *Angew. Chem., Int. Ed.* **1992**, *31*, 1622. (d) Piguet, C.; Hopfgartner, G.; Williams, A. F.; Bunzli, J. C. *Chem. Commun.* **1995**, 491.

(18) Lehn, J. M.; Rigault, A.; Siegel, J.; Harrowfield, J.; Chevrier, B.; Moras, D. *Proc. Natl. Acad. Sci. U.S.A.* **1987**, *84*, 2565.

(19) (a) Rowan, A. E.; Nolte, R. J. M. *Angew. Chem., Int. Ed.* **1998**, *37*, 63. (b) Zheng, X. D.; Lu, T. B. *CrystEngComm* **2010**, *12*, 324. (c) Piguet, C.; Bernardinelli, G.; Hopfgartner, G. *Chem. Rev.* **1997**, *97*, 2005. (d) Albrecht, M. *Chem. Rev.* **2001**, *101*, 3457.

(20) (a) Wei, K. J.; Ni, J.; Min, Y. Z.; Chen, S. M.; Liu, Y. Z. *Chem. Commun.* **2013**, *49*, 8220. (b) Tan, X.; Zhan, J. X.; Zhang, J. Y.; Jiang, L.; Pan, M.; Su, C. Y. *CrystEngComm* **2012**, *14*, 63. (c) Chen, K.; Hu, Y. F.; Xiao, X.; Xue, S. F.; Tao, Z.; Zhang, Y. Q.; Zhu, Q. J.; Liu, J. X. *RSC Adv.* **2012**, *2*, 3217. (d) Peng, G.; Ma, L.; Cai, J. B.; Liang, L.; Deng, H.; Kostakis, G. E. *Cryst. Growth Des.* **2011**, *11*, 2485. (e) Dura, G.; Carrion, M. C.; Jalon, F. A.; Rodriguez, A. M.; Manzano, B. R. *Cryst. Growth Des.* **2013**, *13*, 3275. (f) Katsuki, I.; Motoda, Y.; Sunatsuki, Y.; Matsumoto, N.; Nakashima, T.; Kojima, M. *J. Am. Chem. Soc.* **2002**, *124*, 629. (g) Xu, Y. H.; Lan, Y. Q.; Wu, S. X.; Shao, K. Z.; Su, Z. M.; Liao, Y. *CrystEngComm* **2009**, *11*, 1711. (h) Ding, S.; Gao, Y. F.; Ji, Y. F.; Wang, Y. Q.; Liu, Z. L. *CrystEngComm* **2013**, *15*, 5598. (i) Liu, Q. Y.; Wang, Y. L.; Zhang, N.; Jiang, Y. L.; Wei, J. J.; Luo, F. *Cryst. Growth Des.* **2011**, *11*, 3717. (j) Yang, Q. X.; Chen, Z. J.; Hu, J. S.; Hao, Y.; Li, Y. Z.; Lu, Q. Y.; Zheng, H. G. *Chem. Commun.* **2013**, *49*, 3585. (k) Cai, S. L.; Zheng, S. R.; Wen, Z. Z.; Fan, J.; Zhang, W. G. *Cryst. Growth Des.* **2012**, *12*, 2355. (l) Gao, M. J.; Yang, P.; Cai, B.; Dai, J. W.; Wu, J. Z.; Yu, Y. *CrystEngComm* **2012**, *14*, 1264. (m) Liu, G. N.; Lin, J. D.; Xu, Z. N.; Liu, Z. F.; Guo, G. C.; Huang, J. S. *Cryst. Growth Des.* **2011**, *11*, 3318. (n) Yuan, G.; Shao, K. Z.; Wang, X. L.; Lan, Y. Q.; Du, D. Y.; Su, Z. M. *CrystEngComm* **2010**, *12*, 1147. (o) Chen, H. F.; Guo, G. C.; Wang, M. S.; Xu, G.; Zou, W. Q.; Guo, S. P.; Wu, M. F.; Huang, J. S. *Dalton Trans.* **2009**, 10166. (p) Zhang, L. M.; Deng, D. Y.; Peng, G.; Sun, L.; Liang, L.; Lan, G. Q.; Deng, H. *CrystEngComm* **2012**, *14*, 8083. (q) Zhang, H. B.; Wu, S. T.; Tian, C. B.; Lin, Z. J.; Li, Z. H.; Lin, P.; Du, S. W. *CrystEngComm* **2012**, *14*, 4165. (r) Chen, S. C.; Zhang, J.; Yu, R. M.; Wu, X. Y.; Xie, Y. M.; Wang, F.; Lu, C. Z. *Chem. Commun.* **2010**, *46*, 1449. (s) Wang, M. X.; Long, L. S.; Huang, R. B.; Zheng, L. S. *Chem. Commun.* **2011**, *47*, 9834.

(21) Sheldrick, G. M. *SADABS (the Siemens Area Detector Absorption Correction)*; University of Göttingen: Göttingen, Germany, 2005.

(22) Sheldrick, G. M. *Acta Crystallogr.* **2008**, *A64*, 112.

(23) (a) Moore, J. W.; Glick, M. D.; Baker, W. A., Jr. *J. Am. Chem. Soc.* **1972**, *94*, 1858. (b) Shuangxi, L.; Linpei, J. *Beijing Shifan Daxue Xuebao, Ziran Kexueban* **1996**, *32*, 96. (c) Fupei, L.; Ruixiang, H.; Yi, Y.; Xianlan, T.; Enting, P.; Zhongyuan, Z. *J. Guangxi Norm. Univ.* **1998**, *16*, 38. (d) Chen, W.; Fukuzumi, S. *Inorg. Chem.* **2009**, *48*, 3800. (e) Prout, K.; Marin, J. M.; Hutchison, C. A., Jr. *Acta Crystallogr.* **1985**, *C41*, 201. (f) Jin, Q.-H.; Li, X.; Zou, Y.-Q.; Yu, K.-B. *Cryst. Struct.* **2003**, *218*, 45. (g) Yan, B.; Xie, Q. *J. Coord. Chem.* **2003**, *56*, 1285. (h) Jia, G.; Law, G.-L.; Wong, K.-L.; Tanner, P. A.; Wong, W.-T. *Inorg. Chem.* **2008**, *47*, 9431.

(24) Benelli, C.; Gatteschi, D. *Chem. Rev.* **2002**, *102*, 2369.

(25) Evangelisti, M.; Roubeau, O.; Palacios, E.; Camón, A.; Hooper, T. N.; Brechin, E. K.; Alonso, J. J. *Angew. Chem., Int. Ed.* **2011**, *50*, 6606.